STABILITY ANALYSIS OF CLOSED-LOOP INPUT SHAPING CONTROL

John R. Huey **William Singhose**

Georgia Institute of Technology
J. Huey – gt0241a@prism.gatech.edu
W. Singhose – bill.singhose@me.gatech.edu

Abstract: Input shaping is a vibration control technique that operates by filtering reference commands so that the modified (or shaped) command does not excite the system's natural frequencies. Usually, input shaping is limited to a filtering operation outside of any feedback loops. However, this implementation prevents input shaping from effecting some vital control applications including disturbance rejection, initial condition response, etc. Therefore, some research has suggested using input shapers within feedback loops. This paper will present some initial investigations toward the fundamental understanding of how input shapers utilized within feedback loops affect closed loop stability.

Keywords: Command Shaping, Stability, Input Shaping

1. INTRODUCTION

The vibratory control of flexible systems is an immense field of research. Consequently, there are many types of vibration control, including PID control, optimal control, filters, etc. These control strategies are utilized in a variety of control architectures, e.g. open-loop control, feedback control, or feed-forward control. One effective and well-known form of vibration control is input shaping (Singer and Seering [1990]). This type of command shaping control has been widely used, including applications to cranes (Singer et al. [1997]), coordinate measuring machines (Singhose et al. [1996]), spacecraft (Singh and Vadali [1993]), and long reach robots (Magee and Book [1995]).

1.1 Outside-the-Loop Input Shaping Review

Input shaping works by convolving a standard reference command with a series of impulses specifically designed to eliminate unwanted vibratory modes. Figure 1 depicts this process by showing a step command convolved with a two-impulse shaper to produce a staircase command that results in zero vibration.

Traditionally, input shaping has been used outside the feedback control loop. Utilizing input shaping in this way prevents it from directly addressing some important vibration control issues such as disturbances, non-zero initial conditions, actuator saturation, etc. However, considering the overall simplicity of input shaping (from both a theoretical and practical/implementation perspective) it is certainly desirable to investigate whether or not input shaping can address these phenomena by including it inside feedback loops.

Another way to view input shaping is to analyze it in the Laplace domain (Bhat and Miu [1990]). Here, an input shaper is designed to cancel a system's stable poles with the zeros inherent to the shaper. For instance, a "Zero Vibration" (ZV) shaper (Smith [1957]), like the one shown in

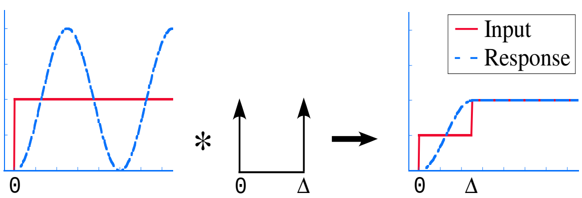

Fig. 1. Input Shaping Procedure.

Figure 1, contains two impulses. The first impulse occurs at time $t = 0$ with a magnitude of A_1. The second impulse, which has a magnitude of A_2, occurs at some delayed time. In the laplace domain, the equation for a ZV shaper is:

$$I_{ZV}(s) = A_1 + A_2 e^{-st_2} \tag{1}$$

Using $s = \sigma + j\omega$, one can solve for the zeros of I_{ZV}. This will lead to two separate equations that must be simultaneously satisfied.

$$\frac{A_1}{A_2} = e^{-\sigma t_2} \tag{2}$$

$$-1 = e^{-i\omega t_2} \tag{3}$$

One solution to these equations is $\omega = \frac{\pi}{t_2}$ and $\sigma = -\frac{1}{t_2} ln \frac{A_1}{A_2}$.

If this shaper is to cancel a set of damped poles, then $\omega = \omega_d$ (where ω_d is the system's damped natural frequency). In other words, $t_2 = \frac{\pi}{\omega_d}$. Also, A_1 and A_2 must now be set so that $\sigma = -\zeta\omega_n$, where ζ and ω_n are the damping ratio and natural frequency of the system.

One interesting note that will become important when input shapers are included within feedback loops is that this ZV shaper has an infinite number of zeros. From (3) it is evident that ωt_2 can actually be any odd multiple of π. Therefore,

$$\omega = \frac{\pm n\pi}{t_2} \qquad (where \quad n = 1, 3, 5, ...) \tag{4}$$

will satisfy (3). This means that an input shaper actually establishes an infinite column of zeros, with the first zero usually set to cancel the poles of the flexible system. This can be seen in Figure 2, which shows the open-loop zeros of an input shaper designed for $\omega_n = 2\pi, \zeta = 0$.

Lastly, it is important to note that a ZV shaper has no finite, open-loop poles. Only when the real part of s is $-\infty$ ($s = -\infty + j\omega$) does $I_{ZV} = \infty$ in the laplace domain.

1.2 Closed-Loop Input Shaping

While feedback oriented control problems have typically been dealt with via PID control and other classical methods, some work has used input shapers inside of feedback loops (Calvert and Sze [1961], Drapeau and Wang [1993], Kapila et al. [2000], Smith [1958], Staehlin and Singh [2003], Sze and Calvert [1955], Zuo et al. [1995], Zuo and Wang [1992]). For instance, Kapila, *et al.* designed a closed-loop input shaping (CLIS) control system to perform well despite modelling errors and errors in the timing of the shaper impulses (Kapila et al. [2000]). Zuo, *et al.* and Drapeau, *et al.* designed their own CLIS scheme (Drapeau and Wang [1993], Zuo et al. [1995], Zuo and Wang [1992]). They experimentally compared it to PID control combined with outside-the-loop input shaping. Finally, they experimentally

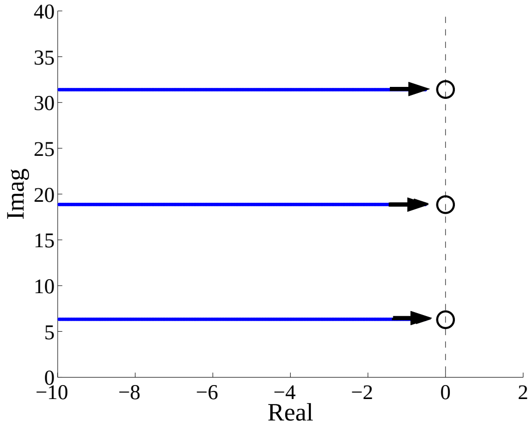

Fig. 2. ZV Shaper Inside a Feedback Loop.

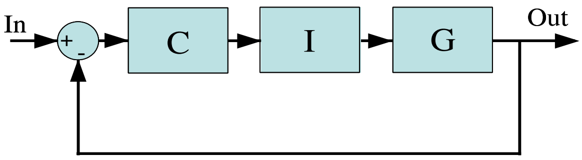

Fig. 3. Basic CLIS Block Diagram.

demonstrated their CLIS controller's ability to reject disturbances.

The most obvious form of closed-loop input shaping would look like the block diagram shown in Figure 3. Here, C is some feedback controller, G is the plant, and I is an input shaper designed to cancel the poles of G. This is the form most often found in the literature.

Considering input shaping's success in open-loop vibration control, it is natural to think that it has potential to improve a system's response to disturbances, non-zero initial conditions, etc. However, the presence of time delays within a feedback loop presents an obvious question of closed-loop stability. Unfortunately, the literature lacks an in depth presentation and understanding of the stability of feedback systems utilizing input shapers inside the loop. Although, there are a few basic guidelines for achieving closed-loop stability. For instance, when analyzing a special class of manipulators, Zuo et. al. established, via a Nyquist analysis, a desired relationship between the system's crossover frequency (ω_c) and frequency of vibration (ω_n) to ensure closed-loop stability (Zuo et al. [1995], Zuo and Wang [1992]). Kapila, et. al., used Lyapunov stability criterion to show that their particular CLIS strategy will be asymptotically stable (Kapila et al. [2000]). Finally, Staehlin and Singh, who analyzed an undamped, second-order system, discussed closed-loop stability in terms of the relationship between the modelled and actual system frequencies (Staehlin and Singh [2003]).

This paper intends to broaden and deepen the understanding of closed-loop input shaping from a stability standpoint. This paper will focus on the CLIS scheme described in Figure 3, as it is the most intuitive realization and is the form most often found in literature. The main goals are to understand how various system parameters (damping, natural frequency, proportional gain, and some classical feedback controllers) affect the system stability. In addition, modelling errors will be included in this stability study.

2. ROOT LOCUS AND BODE DIAGRAM

To begin our investigation of CLIS control, it is important to first understand the basic affects of adding an input shaper inside a feedback loop. For example, what would the root locus and Bode diagram of Figure 3 look like if the plant, G, was removed and the controller, C, was just a proportional gain, K? Figure 2 shows the root locus of a such a system, with the ZV shaper designed to cancel the oscillatory dynamics $\omega_n = 2\pi$ and $\zeta = 0$. Note that Figure 2, as well as the remaining root locus plots within this paper, only show the closed-loop poles up to a finite K value. In addition, for simplicity's sake, all root locus plots in this paper are restricted to quadrants one and two of the imaginary plane. The main point to notice from Figure 2, is that when input shapers are included within feedback loops, they will introduce oscillatory, closed-loop poles. Depending upon the exact control scheme used, these dynamics (arising purely from the input shaper) can be a significant source of oscillatory and/or unstable dynamics for the overall closed-loop system.

Another way to analyze this effect is with the open-loop Bode diagram. The Bode diagram of a ZV shaper, again tuned for $\omega_n = 2\pi$ and $\zeta = 0$, is shown in Figure 4. The discontinuity in the phase plot of the input shaper is a consequence of the shaper zeros lying directly on the imaginary axis (Figure 2). In terms of the Nyquist plot, this results in vectors of magnitude zero (i.e. the angle is undefined), and hence the phase discontinuities.

3. CLOSED-LOOP STABILITY WITH A SECOND-ORDER PLANT

A second-order system is relatively simple, yet it can give important insight into more complicated systems. Therefore, it is useful to study the stability issues inherent to the control system shown in Figure 3 when

$$G = \frac{\omega_n^2}{s^2 + 2\zeta\omega_n s + \omega_n^2}. \tag{5}$$

3.1 Natural Frequency Modelling Error

In order to study the effects of modelling error, the plant natural frequency will be defined as ω_n and the frequency used to design the shaper will be defined as ω_s. Note that the controller, C, is just a proportional controller ($C = K$). If the shaper is exactly tuned to the plant frequency, then the root locus will be similar to that shown in Figure 5. Here again, the plant parameters are $\omega_n = 2\pi$ and $\zeta = 0$.

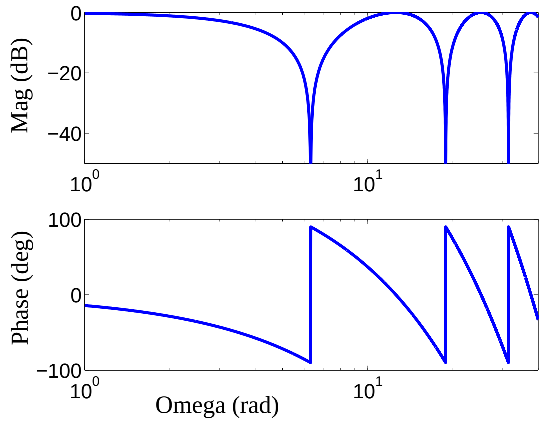

Fig. 4. Bode Diagram of a ZV Shaper.

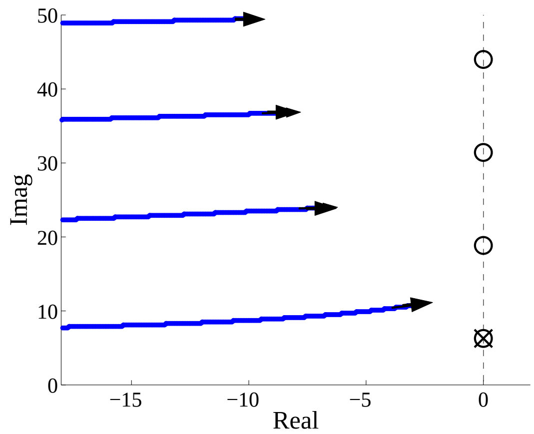

Fig. 5. Root Locus with pole/zero cancellation.

Examining the effects of modelling error, a basic pattern begins to emerge. If $\omega_n < \omega_s$, then the root locus is as shown in Figure 6. Clearly, the root locus branch extending from the plant poles goes unstable immediately. However, if $\omega_n > \omega_s$, this branch remains stable. This can be seen in the Figure 7.

This pattern continues as the plant pole is moved along the imaginary axis. When the pole is below the shaper zero to which it is closest, the branch extending from the plant pole is unstable. However, when the pole is above the zero to which it is closest, then the branch extending from the plant pole is initially stable. Note that Staehlin and Singh found a similar oscillating stability result in their CLIS control scheme (Staehlin and Singh [2003]).

3.2 Effects of K, ζ, and Lead Compensator

By increasing the gain, this system will eventually be driven unstable in all cases. For example, Figure 7 shows a system, with some modelling error, that is initially stable. However, as shown in Figure 8, when K is further increased, the root locus branches arising from the input shaper go unstable. This is an excellent example of the impact that the input shaper can have on the closed-loop system. While the dynamics arising from the plant were always stable, it was the

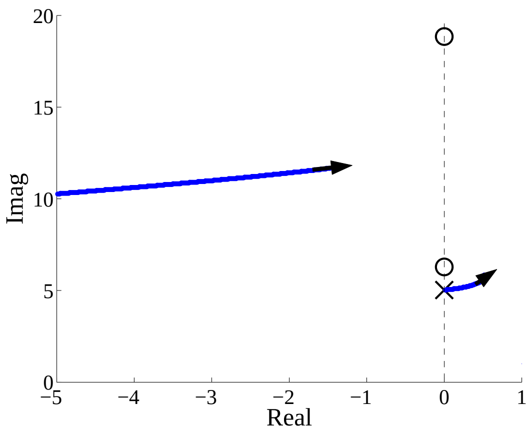

Fig. 6. Root Locus where $\omega_n < \omega_s$.

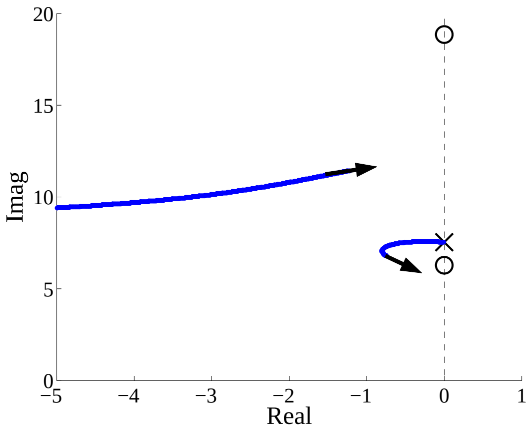

Fig. 7. Root Locus where $\omega_n > \omega_s$.

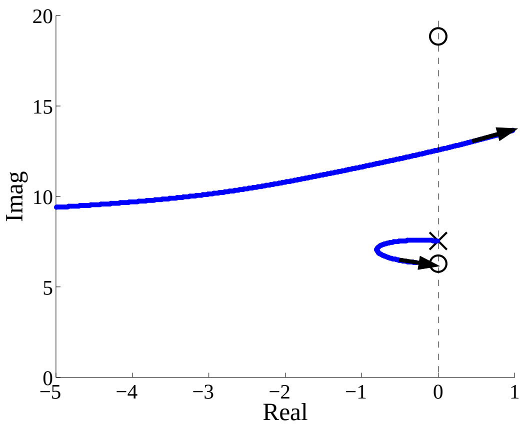

Fig. 8. Root Locus with High K Value.

input shaper's dynamics that eventually drove the closed-loop system unstable.

When the second-order plant has damping, the regions of stability are increased. Figure 9 shows this effect on a root locus plot. By increasing ζ, the root locus branches are shifted to the left.

Including a lead compensator in the controller,

$$C = K\frac{s+z}{s+p}, \tag{6}$$

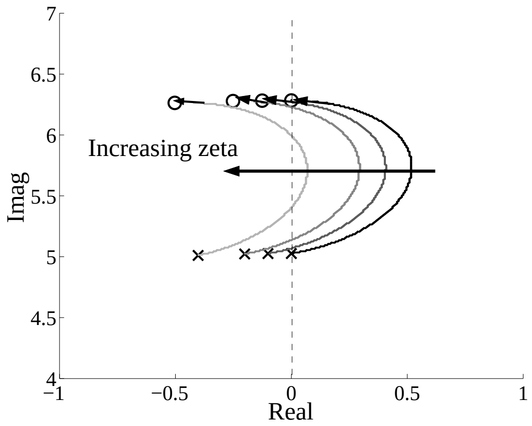

Fig. 9. Effect of Increased System Damping.

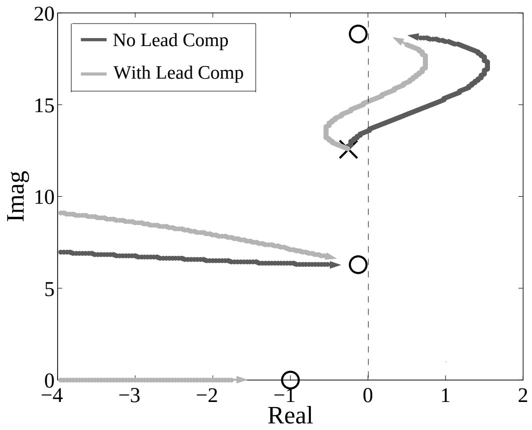

Fig. 10. Influence of Lead Compensator.

adds even more stability to the closed-loop system. Figure 10 shows how the root locus branches are pulled to the left by the lead compensator dynamics. Therefore, increasing ζ or adding a lead compensator will allow the closed-loop system to have larger K values and/or larger modelling errors and yet still remain stable.

4. FOURTH-ORDER SYSTEM

In order to analyze a more complicated system, the damped mass-spring-mass system shown in Figure 11 was investigated. Here, only collocated control was analyzed. The block diagram of the control system is depicted in Figure 12. The transfer functions $\frac{X}{F}$ and $\frac{Y}{X}$ are:

$$\frac{X}{F} = \frac{1}{M_1}\frac{s^2 + 2\zeta_2\omega_2 s + \omega_2^2}{s^2(s^2 + 2\zeta_1\omega_1 s + \omega_1^2)} \tag{7}$$

$$\frac{Y}{X} = \frac{2\zeta_2\omega_2 s + \omega_2^2}{s^2 + 2\zeta_2\omega_2 s + \omega_2^2} \tag{8}$$

where:

$$\omega_1 = \sqrt{K\frac{M_1 + M_2}{M_1 M_2}} \qquad \omega_2 = \sqrt{\frac{K}{M_2}} \tag{9}$$

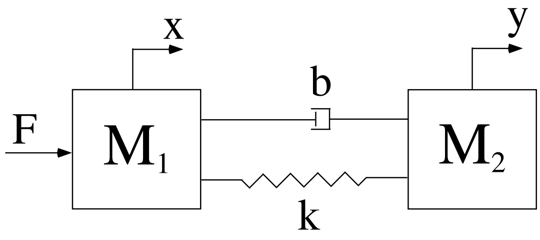

Fig. 11. Mass-Spring-Mass System.

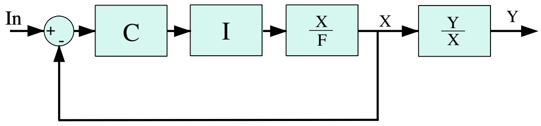

Fig. 12. Block Diagram of Collocated System.

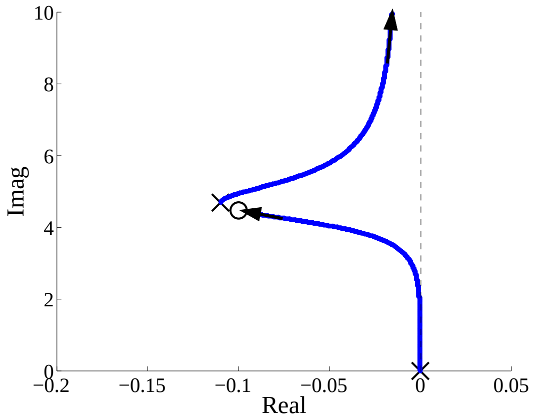

Fig. 13. Root Locus without Input Shaper.

$$2\zeta_1\omega_1 = b\frac{M_1 + M_2}{M_1 M_2} \qquad 2\zeta_2\omega_2 = \frac{b}{M_2} \tag{10}$$

Because the input shaper is included within the feedback loop, it is designed to cancel the open-loop dynamics of $\frac{X}{F}$. Therefore, since $\frac{X}{F}$ has only one open-loop, oscillatory mode (ω_1, ζ_1), a single mode *ZV* shaper was chosen.

4.1 Root Locus Analysis

When the closed-loop system shown in Figure 12 is simplified so that it contains no input shaper and has only a proportional gain, the system's root locus is as shown in Figure 13. Clearly, this system is closed-loop stable. Note that, assuming both (ω_1, ζ_1) and (ω_2, ζ_2) form underdamped dynamics, the root locus shown in Figure 13 is one of only two possible basic shapes - both of which are stable.

If an input shaper is added to the closed-loop system, then the root locus becomes as shown in Figure 14. Even with small K values, the system is unstable. However, if C contains a lead compensator in addition to proportional control, then stability can be achieved. An example of this effect is shown in Figure 15. As a result of adding the lead compensator, this root locus shows large regions of stability.

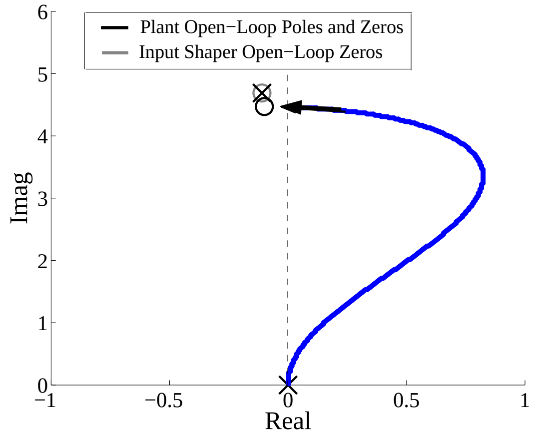

Fig. 14. Root Locus of Complete Control System.

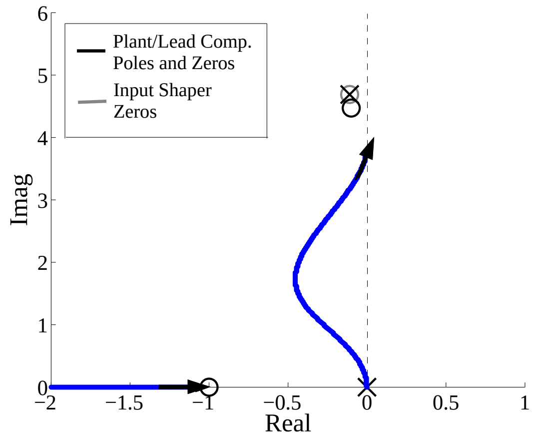

Fig. 15. Root Locus with a Lead Compensator.

4.2 Modelling Errors

To verify the general stability of closed-loop input shaping of a fourth-order system with a lead compensator, the effect of modelling errors was analyzed. If the complex poles of $\frac{X}{F}$ are perfectly modelled, then the ZV shaper could theoretically be tuned such that full pole/zero cancellation occurs. This is shown in Figures 14 and 15. However, this exact modelling is never possible. For the case where the shaper frequency (ω_s) is smaller than the plant frequency (ω_1), the resulting root locus can be seen in Figure 16. As expected from the study of second-order systems, this scenario results in a root locus branch from the plant pole that departs to the left. This scenario usually does not greatly decrease stability. However, if the shaper frequency is larger than the plant frequency, then the root locus branch originating from the plant pole departs to the right (as shown in Figure 17). With second-order systems, this scenario often caused significant stability problems. However, in this fourth-order system, the plant pole is now located between two zeros - one from the input shaper and one from the plant's numerator dynamics. For this reason, stability is not degraded to the extent seen in second-order systems. According to Figure 17, even for large

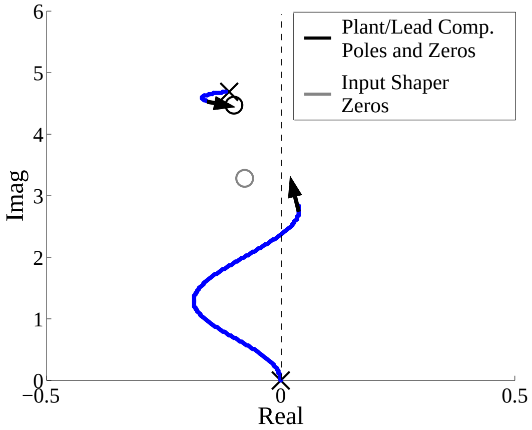

Fig. 16. Root Locus of System with $\omega_s < \omega_1$.

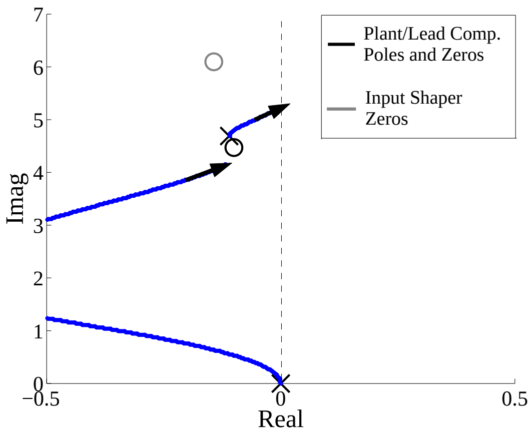

Fig. 17. Root Locus of System with $\omega_s > \omega_1$.

values of K, the root locus branch extending from the plant pole remains stable.

5. CONCLUSIONS AND FUTURE WORK

While some previous research has demonstrated the effectiveness of closed-loop input shaping (e.g. disturbance rejection), this paper has presented an in depth stability study of closed-loop input shaping control. The analysis has shown, from a classical controls perspective, why a CLIS controller often has stability problems, what parameters often influence instability, and how CLIS controllers can be made stable even in the presence of modelling errors.

While this paper examined only 2^{nd} and 4^{th}-order systems, one can extrapolate some preliminary guidelines for designing a CLIS control system of the form shown in Figure 3. Of primary importance is to recognize that an input shaper within the feedback loop will add its own poles to the closed-loop system. Therefore, even if the closed-loop poles arising from the plant open-loop poles remain stable, the overall closed-loop system can still be unstable. Fortunately, some basic control system properties still hold in the case of CLIS. That is, high gains tend to result in instability, but damping and stability enhancing controllers (i.e. lead compensators) improve stability.

A preliminary procedure for designing CLIS schemes would be to use a Root Locus or Bode analysis tool to observe the closed-loop system's full dynamics and adjust system parameters based upon the knowledge of their effect to ensure closed-loop stability within a desired range of parameter uncertainty or variation.

Future work is needed to extend this understanding to other common systems and to other forms of CLIS, as well as to experimentally verify the findings presented in this paper.

6. ACKNOWLEDGEMENTS

The authors would like to thank Northrop-Grumman for their support of this project.

REFERENCES

S. P. Bhat and D. K. Miu. Precise point-to-point positioning control of flexible structures. *J. of Dynamic Sys., Meas., and Control*, 112(4):667–674, 1990.

John F. Calvert and Tsung W. Sze. Short-time memory devices in closed-loop systems, Nov. 21, 1961 1961.

Vincent Drapeau and David Wang. Verification of a closed-loop shaped-input controller for a five-bar-linkage manipulator. In *IEEE Conf. on Robotics and Automation*, pages 216–221, Atlanta, Ga, 1993.

Vikram Kapila, Anthony Tzes, and Qiguo Yan. Closed-loop input shaping for flexible structures using time-delay control. *Journal of Dynamic Systems, Measurement, and Control*, 122:454–460, September 2000.

David P. Magee and Wayne J. Book. Filtering micro-manipulator wrist commands to prevent flexible base motion. In *American Control Conf.*, pages 924–928, Seattle, WA, 1995.

Neil Singer, William Singhose, and Eric Kriikku. An input shaping controller enabling cranes to move without sway. In *ANS 7th Topical Meeting on Robotics and Remote Systems*, volume 1, pages 225–231, Augusta, GA, 1997.

Neil C. Singer and Warren P. Seering. Preshaping command inputs to reduce system vibration. *J. of Dynamic Sys., Measurement, and Control*, 112(March): 76–82, 1990.

T. Singh and S. R. Vadali. Input-shaped control of three-dimensional maneuvers of flexible spacecraft. *J. of Guidance, Control, and Dynamics*, 16(6):1061–8, 1993.

William Singhose, Neil Singer, and Warren Seering. Improving repeatability of coordinate measuring machines with shaped command signals. *Precision Engineering*, 18(April):138–146, 1996.

O. J. M. Smith. Posicast control of damped oscillatory systems. *Proceedings of the IRE*, 45(September):1249–1255, 1957.

O. J. M. Smith. *Feedback Control Systems*. McGraw-Hill Book Co., Inc., New York, 1958.

U. Staehlin and T. Singh. Design of closed-loop input shaping controllers. In *American Control Conference*, pages 5167–5172, Denver, Co, June, 2003 2003.

Tsung W. Sze and John F. Calvert. Short-time memory devices in closed-loop system – steady-state response. In *AIEE Fall General Meeting*, pages 340–344, Chicago, Ill., October 1955.

Kai Zuo, Vincent Drapeau, and David Wang. Closed loop shaped-input strategies for flexible robots. *The International Journal of Robotics Research*, 14(5):510–529, October 1995.

Kai Zuo and David Wang. Closed loop shaped-input control of a class of manipulators with a single flexible link. In *IEEE International Conference on Robotics and Automation*, pages 782–787, Nice, France, May 1992.